

Temperatures in heavy ion reactions: Simulation via quasiparticle dynamics

David H. Boal, James N. Glosli, and Cameron Wicentowich

Department of Physics, Simon Fraser University, Burnaby, British Columbia, Canada V5A 1S6

(Received 6 April 1989)

The observation of different temperatures obtained in heavy-ion reactions by measuring kinetic energy distributions (kinetic temperatures) or abundances of different species (chemical temperatures) is addressed by means of a computer simulation based on the quasiparticle dynamics model. The simulations qualitatively agree with experiment: For both ${}^4\text{He}$ and ${}^6\text{Li}$ nuclei emitted in intermediate-energy heavy-ion reactions, the chemical temperature is found to be in the 3 ± 1 MeV range, much lower than the kinetic temperature. Further, we do not find a strong variation of the chemical temperatures over the laboratory bombarding energy range of $35A$ to $100A$ MeV. The difference in the two temperatures is found to be established after a fairly short time scale roughly corresponding to the breakup time of the reaction region.

I. INTRODUCTION

The thermal model has been used with success for some years in describing the differential cross sections of particles emitted in heavy-ion reactions.¹ In the thermal model the single-particle kinetic energy spectra are fitted with the functional form associated with a Maxwell-Boltzmann distribution of particles as observed from a moving frame. The fit then yields the velocity of the frame as well as the temperature of the particles.

An alternative approach to this determination of the temperature was proposed several years ago: the measurement of excited-state populations. The first measurement by this means,² which we will refer to as the chemical temperature to distinguish it from the kinetic temperature associated with the energy spectrum analysis, yielded values which were dramatically lower than the kinetic results, in some cases up to a factor of 10 lower. There have been a number of experiments³ since the original measurement which have both verified it and provided other systems whose ratio of chemical to kinetic temperatures are closer to unity, typically about 1:4.

There are a number of factors which could affect the population ratios, which in turn would alter the apparent temperature. One difficulty is that excited-state decays on a time scale much longer than the typical time frame of a few times 10^{-22} sec associated with the reaction will also change the populations.⁴ For example, a more detailed analysis of excited state decays raised the apparent temperature of $\frac{1}{2}$ -1 MeV found in Ref. 2 for lithium nuclei considerably.⁵ However, even when these decays are taken into account (admittedly in a model-dependent way), the difference between the kinetic and chemical temperatures remains.

On general grounds we do not expect these two methods of temperature measurement to yield the same results. The distribution of kinetic energies is determined relatively early in the reaction and is mainly a function of the bombarding energy and geometry, the latter through the multiplicity of noncompound reaction products and

the equipartition theorem. However, as the thermalized spatial region in a collision expands, the temperature observed in a frame comoving with a local region of coordinate space will decrease.⁶ As long as a given species remains in chemical equilibrium, the population ratios will follow this locally decreasing temperature.⁷

We recently⁸ begin an investigation of this problem on a more quantitative basis than was possible previously (e.g., Ref. 7) using a computer simulation which possesses stable computational ground states and thus allows the calculation of excitation energy distributions. The details of the simulation, which we refer to as quasiparticle dynamics (QPD), can be found in Ref. 9. The essence of the model is that it uses a momentum-dependent potential—which we refer to as the Pauli potential—to incorporate the antisymmetrization effects inherent to fermions. Thus one works completely within a consistent Hamiltonian formalism both for determining nuclear ground states and propagating those states during a collision.

In Ref. 8 we found that the chemical temperatures were indeed much lower than the kinetic ones for ${}^4\text{He}$ nuclei emitted at wide angles. In this paper we wish to show the full angle and energy dependence of the results, as well as extend them to include lithium nuclei. The plan of the paper is as follows. In Sec. II we will review the techniques used for determining the excitation energy distributions, and obtain results for both ${}^4\text{He}$ and ${}^6\text{Li}$ computational nuclei. These distributions will be applied in Sec. III to the $\text{Ca} + \text{Ca}$ reaction at $35A$ and $100A$ MeV and $b=0$ fm to determine the chemical and kinetic temperatures. Questions such as goodness of fit, determination of errors, etc., are also dealt with in this section. Our conclusions are summarized in Sec. IV.

II. EXCITATION ENERGY DISTRIBUTIONS

In order to determine a temperature from the excitation energy distribution of a given fragment mass we must calculate these distributions as a function of temperature for the nuclei in equilibrium. This is difficult to

evaluate in general because of the presence of the complex nuclear and Pauli potentials. Hence we will use a Monte Carlo procedure to evaluate the excitation energy spectrum. The two nuclei which we will investigate in detail are ${}^4\text{He}$ with all spins paired, and ${}^6\text{Li}$ with total proton and neutron spins equal to $\frac{1}{2}$ [which we will denote by ${}^6\text{Li}(\frac{1}{2}, \frac{1}{2})$]. In particular, the ${}^4\text{He}$ nucleus in which all spins are paired is not subject to the Pauli potential, and can be used to perform numerical checks on our results.

The method we use for the Monte Carlo procedure is the following: an initial configuration is chosen for the quasiparticles representing the nucleons, and then the phase-space coordinate of each quasiparticle is moved successively. The position is moved randomly within a box 0.6 fm to a side centered on the old position, and the momentum is moved in a similar box of dimension 60 MeV/c. After each change, the centers of mass and momentum are positioned to zero and the energy of the new configuration is compared with the old. The configuration is kept if the new energy is lower than the old, or conditionally kept according to the value of a random number compared with the weight $\exp(-\delta E/T)$. After each 50 sweeps through the quasiparticles, the configuration is stored. A total of at least 10 000 configurations is kept at each temperature.

The motivation for sampling every 50 sweeps is the following. Suppose we follow the random walk of a single particle within a box with reflecting walls. The correlation function of the position of the particle as a function of time, $\langle r(t) \cdot r(0) \rangle$ decreases exponentially with a lifetime given approximately by

$$\tau^{-1} = -\ln \cos(\pi/\rho), \quad (1)$$

where ρ is the ratio of box length to average step size. Now in determining how many sweeps should be made between saving configurations, we want successive saved configurations to have little correlation between each other so as to be sure that the Monte Carlo procedure is sampling the total phase space. If we argue that the positions of each quasiparticle should move in a region approximately 2 fm across, then the lifetime given by Eq. (1) corresponds to 35 steps of average length 0.15 fm. Thus the choice of 50 sweeps between saved configurations should produce configurations which are largely uncorrelated. As a numerical check to ensure that the procedure gave reasonable results we also constructed the excitation energy distribution functions described below based upon samples generated every 150 and 500 sweeps. The distributions did not change within the expected statistical error.

There is one technical point worth mentioning which makes a significant difference to the predicted density of states at high temperatures. In the QPD simulation of the reaction, a fragment is defined by searching through the final quasiparticle positions (after an elapsed time of hundreds of fm/c) and linking together those quasiparticles separated in space by less than 3.5 fm. It is important to place the same restrictions on the coordinate positions allowed in the Monte Carlo procedure; otherwise, one will be sampling a very different phase space than

what is used in the reaction simulation.

From the Monte Carlo samples we evaluate the expectation of the kinetic energy per nucleon and the excitation energy per nucleon. The results for the ${}^4\text{He}$ nucleus are shown in Fig. 1. For ${}^4\text{He}$, $\langle E_{\text{KE}}/A \rangle$ can be evaluated analytically, since there is no momentum dependence to the interaction. Then, one would expect that $\langle E_{\text{KE}}/A \rangle = \frac{3}{8} T$, and this is what is obtained from the numerical simulations as well (the proportionality constant is $\frac{3}{8}$ rather than $\frac{1}{2}$ because the c.m. motion is held fixed in the Monte Carlo procedure). As a function of temperature, the excitation energy rises faster than does the kinetic energy because of the presence of the potential term. At low temperature, the displacements of the quasiparticles around their ground-state positions will be small; hence a second-order Taylor expansion of the Hamiltonian in terms of the relative separation is valid. Counting quadratic terms one would expect that $\langle E^*/A \rangle = \frac{3}{4} T$, and again this is what is found in the Monte Carlo results. Similar results can be obtained for ${}^6\text{Li}$ and these are shown in Fig. 2.

Which excitation energy range will be important in determining temperatures will depend on the lifetimes of the excited states. If the lifetimes are too short, then fragments produced with that excitation energy will decay too rapidly and will not be present in any appreciable amounts in the reaction products. Because of this, a temperature based upon the average excitation energy would give misleading results: the high-energy part of the excitation spectrum will decay rapidly with time. Among the products of a heavy-ion collision, there will be few fragments observed with the excitation energies above the

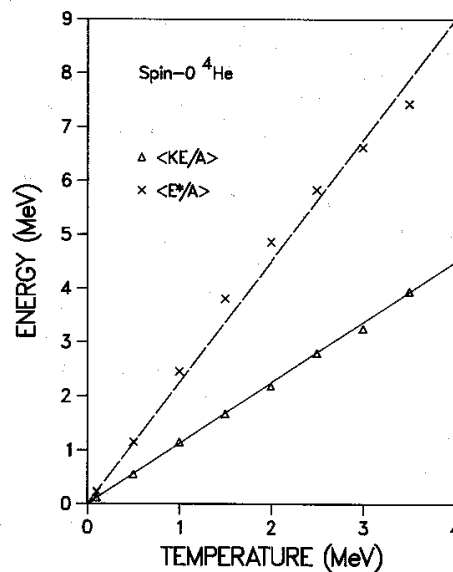


FIG. 1. Calculated kinetic energy per nucleon and excitation energy per nucleon as a function of temperature for computational zero spin ${}^4\text{He}$ nuclei.

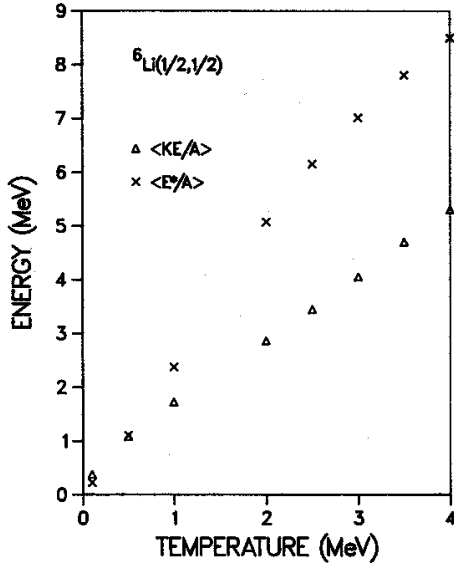


FIG. 2. Calculated kinetic energy per nucleon and excitation energy per nucleon as a function of temperature for computational ${}^6\text{Li}(\frac{1}{2}, \frac{1}{2})$.

threshold for vaporization of the nucleus in question. Of course such fragments will be produced, but they will decay in a very short time frame. In Table I we show some of the threshold energies for different decay channels of the ${}^4\text{He}$ and ${}^6\text{Li}(\frac{1}{2}, \frac{1}{2})$ nuclei. One can see that both nuclei are completely unbound above 7 MeV per nucleon in excitation energy. At lower excitation energies there are a number of decay channels available.

To obtain a quantitative estimate of the lifetimes, the configurations generated in the Monte Carlo simulation of the density of states were grouped according to excitation energy into bins of 1 A MeV and then propagated for 250 fm/c. Each configuration was run through the cluster search routine at 10 fm/c intervals to determine if the cluster had remained connected. Using this method, one could follow the population of a group of excited states and determine their average lifetime. The resulting populations are shown in Fig. 3 as a function of time.

From the figure, one can see that configurations with excitation energy below the decay threshold (3 MeV per nucleon for ${}^4\text{He}$) are stable, as required. At higher excita-

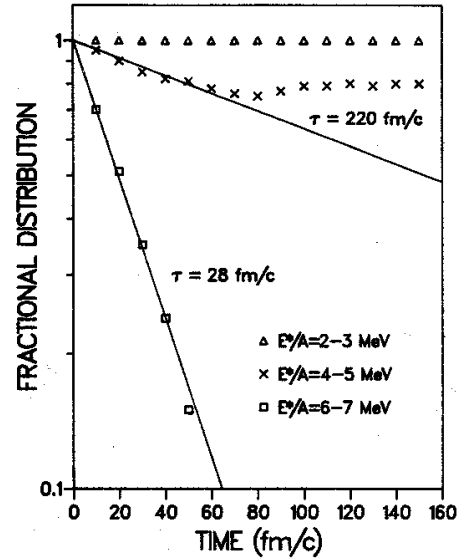


FIG. 3. Time dependence of the population of ${}^4\text{He}$ nuclei with various initial excitation energies: 2A–3A MeV (Δ), 4A–5A MeV (\times) and 6A–7A MeV (\square). The initializations were chosen randomly from the phase space associated with a temperature of 2 MeV subject to the cluster connection constraint.

tions, there is a component which decays in an intermediate time frame (220 fm/c lifetime for the 4–5 MeV per nucleon example) and one component which decays on a very long time scale. Finally, for energies above the vaporization threshold, the configurations are short lived, 28 fm/c in the example shown.

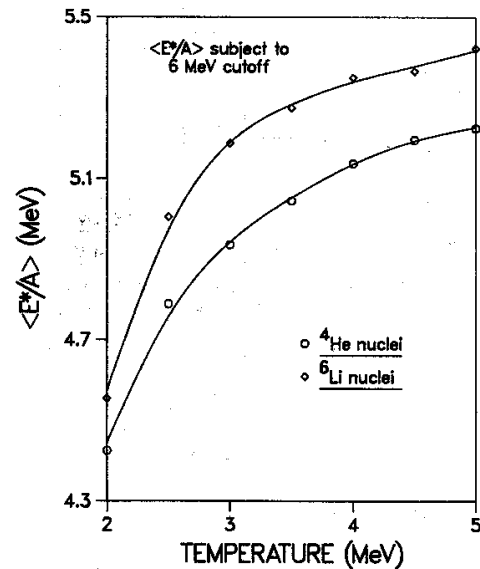


FIG. 4. Calculated average excitation energy per nucleon subject to 6.0 MeV cutoff for ${}^4\text{He}$ and ${}^6\text{Li}$ in their ground-state spin configurations.

TABLE I. Threshold values of the excitation energy per nucleon for selected reactions of computational ${}^4\text{He}$ and ${}^6\text{Li}(\frac{1}{2}, \frac{1}{2})$.

Reaction	E^*/A (MeV)
${}^4\text{He} \rightarrow n + {}^3\text{He}$	3.11
${}^4\text{He} \rightarrow {}^2\text{H} + {}^2\text{H}$	3.53
${}^4\text{He} \rightarrow 2n + 2p$	6.24
${}^6\text{Li} \rightarrow {}^2\text{H} + {}^4\text{He}$	0.99
${}^6\text{Li} \rightarrow {}^3\text{H} + {}^3\text{He}$	1.79
${}^6\text{Li} \rightarrow 3n + 3p$	6.06

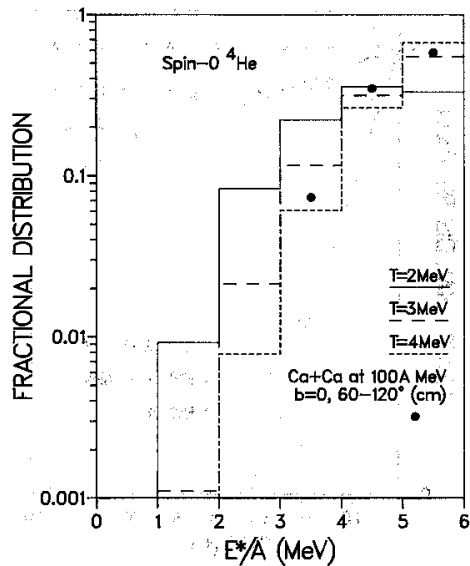


FIG. 5. Fractional distribution of excitation energies per nucleon predicted for the computational zero spin ${}^4\text{He}$ nuclei (subject to cluster constraint) for temperatures of 2, 3, and 4 MeV (histograms). The points are from the simulated Ca+Ca reaction at $100A$ MeV and $b=0$ fm. All distributions have been normalized to unity over the $0A-6.0A$ MeV range in excitation energy. The ${}^4\text{He}$ nuclei were observed in the $60-120$ deg range in the c.m. frame.

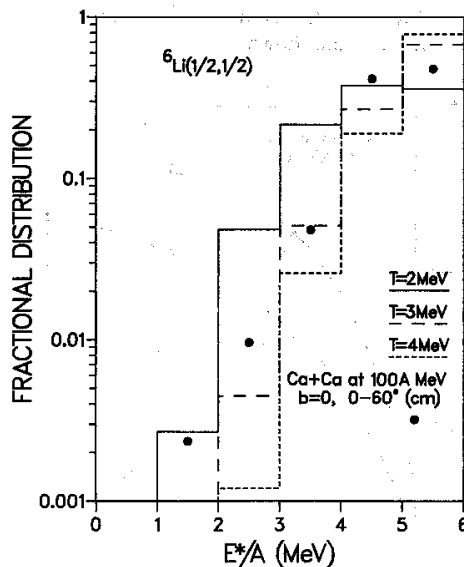


FIG. 6. Fractional distribution of excitation energies per nucleon predicted for the computational ${}^6\text{Li}(\frac{1}{2}, \frac{1}{2})$ nuclei (subject to cluster constraint) for temperatures of 2, 3, and 4 MeV (histograms). The points are from the simulated Ca+Ca reaction at $100A$ MeV and $b=0$ fm. All distributions have been normalized to unity over the $0A-6.0A$ MeV range in excitation energy.

It is clear from this that the part of the excitation energy distribution which will be of most use in reaction studies is the region below $6A$ MeV. States in this energy region will be sufficiently long lived compared to the reaction time (about 100 fm/c) that their spectrum should not be altered appreciably. We plot in Fig. 4 the behavior of the average excitation energies for both ${}^4\text{He}$ and ${}^6\text{Li}(\frac{1}{2}, \frac{1}{2})$ as a function of temperature when the configurations are restricted to have an excitation energy per nucleon of less than 6 MeV. As expected, the determination of the temperature will be less accurate as the average excitation energy per nucleon approaches 5 MeV: in this range the change of the average excitation energy with temperature is slow.

Although we will use these averages when computing the temperature, we also have to ask whether the distributions obtained from the experiments even look like the ones predicted by the Monte Carlo method. To facilitate this comparison, the ${}^4\text{He}$ and ${}^6\text{Li}$ excitation energy distributions are shown in Figs. 5 and 6, respectively, for temperatures of 2, 3, and 4 MeV, the distributions being normalized to unity over the $0-6.0A$ MeV range. As can be seen from the figure, the 2 MeV distribution has a peak below $6A$ MeV and this peak shifts to higher excitation energies as the temperature increases. Although we have not shown the full distributions, they do fall off exponentially at higher excitation energies as is expected.

III. TEMPERATURE DETERMINATION

Having determined the behavior of the excitation energy distributions as a function of temperature, we now evaluate these quantities in a simulated collision. The reaction which we choose to investigate is Ca+Ca at bombarding energies of $35A$ and $100A$ MeV and an impact parameter b of 0 fm. These reactions are assumed to be typical of those for which the temperature measurements have been made. For the $35A$ MeV reaction, a sample of 7000 events was generated, while for the $100A$ MeV reaction, the event sample was 4500. The total event sample including analysis took more than 200 cpu hours to generate on an IBM 3081 mainframe.

The differential cross section which the simulation predicts for the reactions is peaked in the forward and backward directions. The experimental measurements typically have been made away from these regions, so the approach taken here will be to average the fragment angular distributions over two ranges in cm angle: $0-60$ and $60-120$ deg. The predicted ${}^4\text{He}$ and ${}^6\text{Li}$ excitation energy distributions (evaluated at about 100 fm/c after the time of maximum overlap) are shown as data points in Figs. 5 and 6, respectively. In Table II a summary of the number of samples of each nuclide under consideration at time $t=150$ fm/c is shown. This is useful in understanding the errors in the temperature analysis.

The kinetic and chemical temperatures are determined by assuming a Boltzmann distribution, which would be valid if the system was in thermal equilibrium. A maximum likelihood estimate¹⁰ (MLE) \hat{T} is made for both

TABLE II. Summary of sample sizes of ${}^4\text{He}$ and ${}^6\text{Li}$ reaction products for various bombarding energies and emission angles at time $t=150$ fm subject to the cut $E^*/A < 6$ MeV.

Cluster type	Bombarding energy (A MeV)	Sample size between angles		Number of events
		$0^\circ-60^\circ$	$60^\circ-120^\circ$	
${}^4\text{He}$	35	375	27	7000
	100	1191	205	4500
${}^6\text{Li}$	35	80	2	7000
	100	421	49	4500

temperatures. For a Boltzmann distribution the MLE of the kinetic temperature \hat{T}_K is given by

$$\bar{K} \equiv \frac{1}{n} \sum_{i=1}^n K_i = \langle K(\hat{T}_K) \rangle = \frac{3}{2} k_B \hat{T}_K, \quad (2)$$

where K_i is a realization of the center of mass kinetic energy of one of the nuclei in the n -realization sample of like reaction products. Expectations with respect to the Boltzmann distribution are denoted by $\langle \dots \rangle$. The expectation of the kinetic energy can be evaluated and is shown above. The MLE \hat{T}_{E^*} of the chemical temperature is given by

$$\bar{E}^* \equiv \frac{1}{n} \sum_{i=1}^n E_i^* = \langle E^*(\hat{T}_{E^*}) \rangle, \quad (3)$$

where E_i^* is a realization of the excitation energy of one of the nuclei from the n -realization sample of like reaction products subject to the constraint that $E^* < 6.0$ MeV per nucleon. Unlike the kinetic energy, we were unable to obtain an analytic expression for the expectation of the excitation energy, so a Monte Carlo procedure is used to evaluate the right-hand side (rhs) of Eq. (3). As will be shown in more detail below the chemical temperature which is obtained from the above analysis is much lower than the kinetic temperature and is in the range observed experimentally in hadronic decays of ${}^6\text{Li}$ in similar reactions.

From the reaction mechanism point of view, the question of interest is at what time did the chemical and kinetic temperatures begin to differ? Hence, the way we proceed to do the analysis is to stop the simulation every 10 fm/c and perform the same evaluations of the excitation energy distributions as above on whatever clusters are present. Obviously, this approach will yield no information until distinct fragments have begun to emerge from the reaction region. Further, the statistics will not be particularly good for early times in the collision when few fragments are present.

The time dependence of the temperatures is shown in Fig. 7 for ${}^4\text{He}$ emission in the Ca+Ca reaction at 100 A MeV lab bombarding energy. The same angular averages have been performed as before. One can see that the temperatures show little variation after 100 fm/c elapsed reaction time, meaning that their values are fixed near the breakup time. This does not preclude there being a further change in the temperatures arising from long time-frame evaporative emission or other decay processes, but it does indicate that the low chemical temperatures are

set early in the reaction.

The next question which we wish to investigate is the angular dependence of the temperatures. One expects that at forward angles, the average kinetic energies will be higher than at wide angles. Is the same true for the chemical temperatures? The results are shown in Fig. 8(a) for ${}^4\text{He}$ emission. One can see that the chemical temperatures have changed very little, if at all, although the kinetic temperature has risen sharply.

Unfortunately, we do not have sufficiently many events to extract temperatures for ${}^6\text{Li}$ at wide angles because of its lower emission rate. However, there are a sufficiently large number of events to make a comparison at forward angles and this is shown in Fig. 8(b). Again, the chemical temperatures are much lower than the kinetic ones at 100 A MeV bombarding energy. In fact, they are very similar to the ${}^4\text{He}$ results.

One of the other characteristics of the chemical temperatures which was observed experimentally¹¹ was the relative constancy of the temperatures over a range of

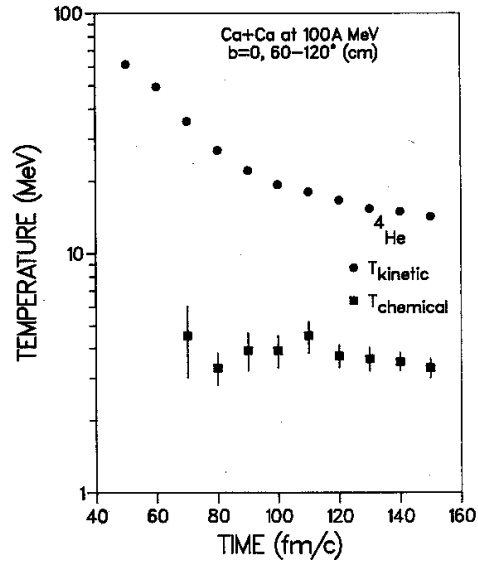


FIG. 7. Time dependence of the ${}^4\text{He}$ kinetic and chemical temperatures calculated for the Ca+Ca reactions at 100 A MeV and $b=0$ fm. The ${}^4\text{He}$ nuclei were collected in the 60–120 deg range in the c.m. frame.

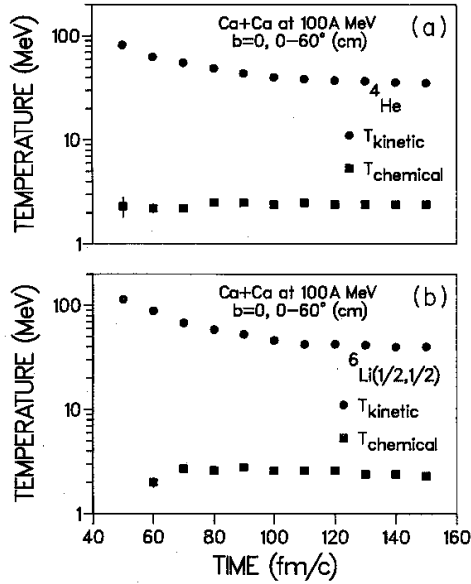


FIG. 8. Time dependence of the kinetic and chemical temperatures for nuclei emitted at 0–60 deg in the Ca+Ca reaction at 100 A MeV. The upper part of the figure (a) is for ${}^4\text{He}$ nuclei while the lower part (b) is for ${}^6\text{Li}(\frac{1}{2}, \frac{1}{2})$.

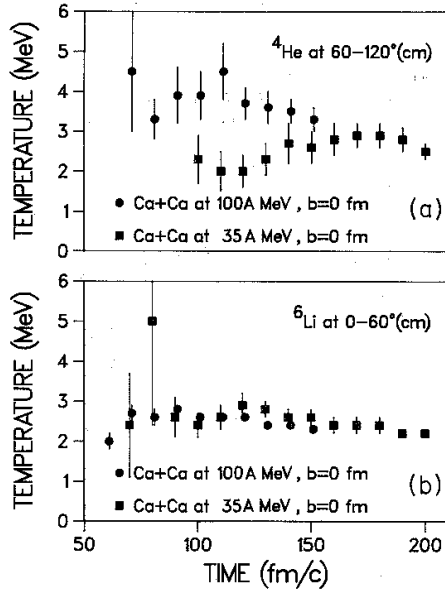


FIG. 9. Comparison of the chemical temperatures obtained in the Ca+Ca reaction at 35 A MeV and 100 A MeV bombarding energy. The top part (a) of the figure is for ${}^4\text{He}$ nuclei in the angular range of 60–120 deg, while the lower part (b) is for ${}^6\text{Li}$ in the angular range of 0–60 deg.

bombarding energies. We ran two bombarding energies for comparison, 35 A and 100 A MeV. As expected, the kinetic temperatures are much lower at 35 A MeV than they are at 100 A MeV. The behavior of the chemical temperatures is shown in Fig. 9. The upper part of the figure shows ${}^4\text{He}$ nuclei emitted in the 60–120 deg range, while the lower part shows ${}^6\text{Li}(\frac{1}{2}, \frac{1}{2})$ emitted in the 0–60 deg range. While the chemical temperatures do rise with bombarding energy, the increase is much smaller than that of the kinetic temperatures.

Although the error bars given by the MLE method allow us to reasonably conclude that the chemical temperature is different from the kinetic one, they do not tell us that the excitation energy distribution itself resembles the equilibrium one at a given temperature. Figures 5 and 6 show that the fit is qualitatively reasonable. However, in order to provide more quantitative information, we performed a chi-square test to the agreement between the reaction data and the equilibrium distributions. As an example, a comparison was made over the 3.0 A–6.0 A MeV region for ${}^4\text{He}$ nuclei in the 60–120 deg range. At each time step we had enough events to make a meaningful assessment, chi squared was generally less than 1 and only occasionally rose as high as 2. This was true for both 35 A and 100 A MeV bombarding energies. Hence we feel that the temperatures determined by the MLE method are indeed meaningful.

IV. DISCUSSION AND SUMMARY

The analysis of the previous section concluded that the chemical temperature as measured by the excited-state populations of ${}^4\text{He}$ and ${}^6\text{Li}(\frac{1}{2}, \frac{1}{2})$ were significantly lower

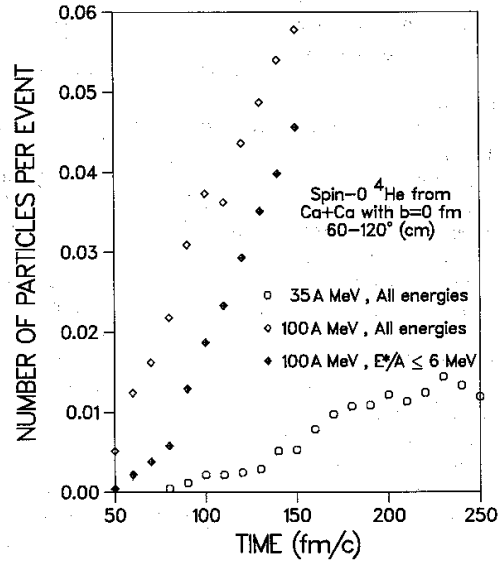


FIG. 10. Time dependence of the number of ${}^4\text{He}$ nuclei per event observed in the angular range of 60–120 deg for the Ca+Ca reaction at 35 A MeV and 100 A MeV bombarding energy. The 100 A MeV populations are shown both with and without the 6 A MeV cut in excitation energy.

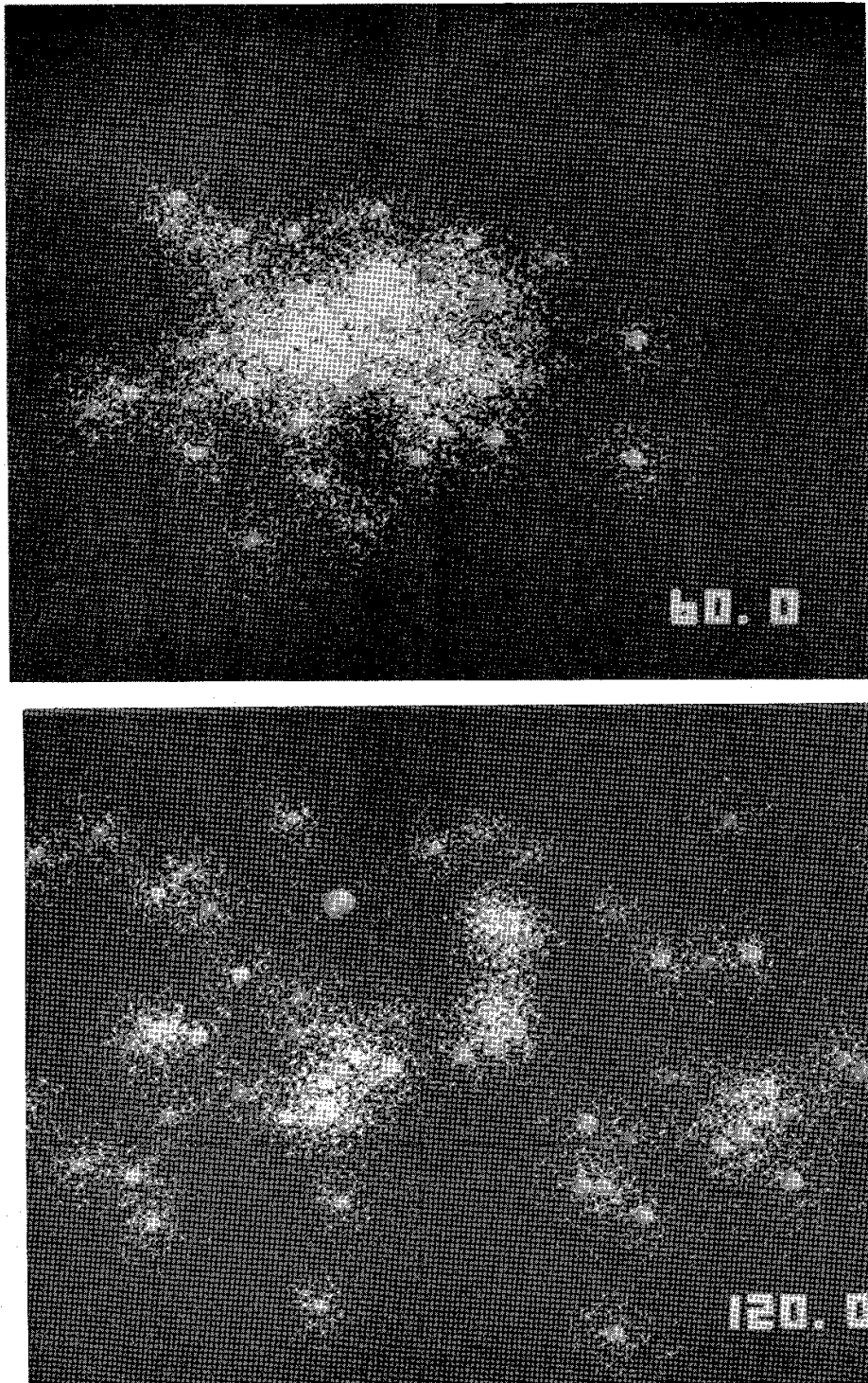


FIG. 11. Representation of the quasiparticle positions in the Ca+Ca reaction at 100.4 MeV and $b=0$ fm. The upper part of the figure is for an elapsed time of 60 fm/c while the lower part is for 120 fm/c.

than the kinetic temperatures extracted from their kinetic energy spectra. The chemical temperature showed only a small variation with emission angle—tending to be lower at forward angles—or with bombarding energy. The magnitude of both temperatures was in the same range as is observed experimentally. One would not expect exact agreement between simulation and experiment, however. One reason is that the reaction is followed only for 150–250 fm/c. This is long enough to ensure that the reaction products are stable on the time scale of hundreds of fm/c, but clearly does not allow for the evaporative emission of particles. Such emissions probably will not change the predicted temperatures by a large amount, particularly the kinetic temperature.

A related but different effect arises from the inequivalent methods of determining the chemical temperature from the simulation and experiment. In the simulation, the excitation energy distribution can be determined at each time step and hence the chemical temperature can be followed as a function of time. For the experimental measurement of the yields of particle unstable nuclei, a time integration is made in the sense that one does not know the emission time of the nuclei that one is reconstructing (for particle unstable nuclei one measures the decay products and reconstructs the population of parent excited states).

Again this is not expected to be a large effect. The population of the excited states in the simulation can be used as a guide to the importance of the time integration. First, Figs. 7–9 show that the chemical temperatures are relatively independent of reaction time; only at early times are they much different from their long-time value. Now, if there were many excited nuclei produced at these early times, then there could be some concern that the time average could be significantly different from the large-time value. Shown in Fig. 10 is the time dependence of the ${}^4\text{He}$ excited-state population, both with and without the 6.4 MeV cut in excitation energy. One can see that at early times, the populations are fairly small. Hence, even if their chemical temperature is different than the large-time value, those nuclei emitted early in the reaction will have only minimal effect on the time average measured experimentally.

Figure 10 also leads us to the last question which we wish to address in this paper: Why are the chemical temperatures so low? It is clear from Fig. 10 that the excited-state population rises as the reaction region expands. To gain some intuition as to what the system looks like as a function of time, we show in Fig. 11 a representation of one event in the Ca+Ca reaction at 100 A MeV. Each quasiparticle is represented by a solid sphere of radius 0.5 fm surrounded by a distribution of points which follows the Gaussian distribution used for the nucleon wave packets. The upper part of the figure shows the system after 60 fm/c; it is clearly highly connected with only a few nucleons and light fragments having separated from the reaction region. The central region expands and breaks up with time, the lower part of the figure showing a sample at 120 fm/c elapsed time.

For such a complicated system it is difficult to distinguish between the breakup of the large reaction region

and the rapid decay of highly excited nuclear droplets. There will be contributions to the fragment spectra from both of these processes. Since many degrees of freedom go out of equilibrium between 150–200 fm/c, we will examine the 50–120 fm/c time region and try to determine the behavior of the local kinetic temperature. Our method is to use the free nucleons (by which we mean those which are not bound in clusters) to determine a local temperature: at each time step those nucleons within 4 fm of the c.m. position of the Ca+Ca system are selected and used to determine the expectation of the transverse kinetic energy averaged over the event sample. The temperature is then taken to be equal to $\langle P_{\perp}^2/2m \rangle$, where P_{\perp} is the transverse momentum. The results are shown in Fig. 12.

Although the average nucleon kinetic energy of the whole spatial region is in the 20 MeV range, for the central region it is much lower, around 3 MeV. One would expect similar results for all local regions once their c.m. motion has been removed. Hence one can see that the chemical temperature is not very different from the local kinetic temperature around breakup stage of the reaction, and we would expect the initial reaction products to have chemical temperatures of about 3 MeV at this time. As the system expands, the local kinetic temperature drops to 2 MeV and below. The number of light fragments continue to increase during this time, and these are likely the result of decay of heavier systems (also initially produced with the low temperatures). In other words, the breakup temperature is in the 3–4 MeV region, and the presence of short-time decays of excited states does

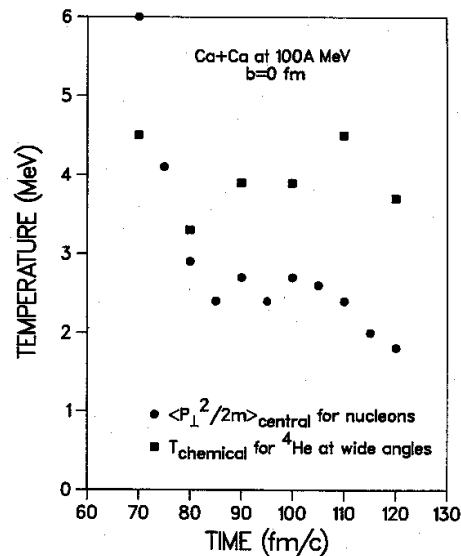


FIG. 12. Time dependence of the free nucleon kinetic temperature in the local reference frame centered on the c.m. position of the reaction system. The reaction chosen is Ca+Ca at 100 A MeV and $b=0$ fm. Shown for comparison is the ${}^4\text{He}$ chemical temperature of Fig. 7.

not change this temperature appreciably.

In summary, we have used a computational model which possesses well-defined nuclear ground states to investigate the problem of temperature measurement in heavy-ion collisions. The model was used to evaluate the fractional distribution of excitation energies as a function of temperature for the computational ^4He and ^6Li nuclei. Next, a simulation was performed of the Ca + Ca reaction at two bombarding energies and fixed impact parameter. The temperatures extracted from this simulation showed the same characteristics as are observed experimentally: the chemical temperature had a value of 2.5–3.5 MeV—much lower than the kinetic temperature—and it varied

only slowly with bombarding energy. Lastly, it was shown that the low value of the chemical temperature is established around the breakup time of the reaction. Decays on the time scale of 10^{-21} sec are not necessary to produce this effect, although they may contribute to it.

ACKNOWLEDGMENTS

The authors wish to thank M. Plischke for several useful discussions. This work was supported in part by the Natural Sciences and Engineering Research Council of Canada.

¹S. Das Gupta and A. Z. Mekjian, *Phys. Rep.* **72**, 131 (1981).

²D. J. Morrissey *et al.*, *Phys. Lett.* **148B**, 423 (1984).

³D. J. Morrissey *et al.*, *Phys. Rev. C* **34**, 761 (1985); C. Bloch *et al.*, *Phys. Rev. C* **34**, 850 (1986); J. Pochodzalla *et al.*, *Phys. Rev. Lett.* **55**, 177 (1985); J. Pochodzalla *et al.*, *Phys. Lett.* **161B**, 275 (1985); for a review, see C. K. Gelbke and D. H. Boal, *Prog. Part. Nucl. Phys.* **19**, 33 (1987); for temperatures obtained from ground-state population ratios, see A. S. Hirsch *et al.*, *Phys. Rev. C* **29**, 508 (1984).

⁴J. Pochodzalla *et al.*, Ref. 3; D. J. Fields *et al.*, *Phys. Lett. B* **187**, 257 (1987); D. Hahn and H. Stocker, *Phys. Rev. C* **35**, 1311 (1987).

⁵C. Bloch *et al.*, *Phys. Rev. C* **36**, 203 (1987).

⁶See, for example, H. Stöcker, J. Hofman, J. A. Maruhn, and W. Greiner, *Prog. Part. Nucl. Phys.* **4**, 133 (1980); J. Aichelin, *Nucl. Phys.* **A411**, 474 (1983).

⁷D. H. Boal, *Phys. Rev. C* **30**, 749 (1984); see also C. Bloch *et al.*, *ibid.* **37**, 2469 (1988).

⁸D. H. Boal, J. N. Glosli, and C. Wicentowich, *Phys. Rev. Lett.* **62**, 737 (1989).

⁹D. H. Boal and J. N. Glosli, *Phys. Rev. C* **38**, 1870 (1988); **38**, 2621 (1988).

¹⁰John E. Freund, *Mathematical Statistics* (Prentice-Hall, Englewood Cliffs, 1971).

¹¹Z. Chen *et al.*, *Phys. Rev. C* **36**, 2297 (1987).